Proceedings of the ASME 2023
International Design Engineering Technical Conferences and
Computers and Information in Engineering Conference
IDETC-CIE2023
August 20-23, 2023, Boston, Massachusetts

DETC2023-116901

ROLL CENTER AND CENTRODES OF AN EIGHT-BAR SUSPENSION SYSTEM

Chiara Lanni, Giorgio Figliolini, Luciano Tomassi

University of Cassino and Southern Lazio, Cassino (Fr), Italy

ABSTRACT

This paper deals with the roll motion analysis of vehicles which are provided of two double wishbone independent suspension mechanisms on the front side. According to a planar car model and supposing that both front wheels are rotating about their fixed revolute joints, the position analysis of an eight-bar mechanism is formulated, in order to determine the position of the roll center, along with the fixed and moving centrodes.

In particular, all instantaneous centers of rotations have been determined by devoting particular attention to the roll center and to those of each wheel with respect to the vehicle chassis, according to the kinematic characteristics of the double wishbone independent suspension mechanism. Moreover, a suitable mechanism with 18 members and 1 d.o.f. is proposed to generate mechanically or by using any CAD-software, both centrodes, according to the direct and inverse planar motion of the chassis with respect to the ground and vice versa. Finally, a first curvature analysis is carried out by using the Euler-Savary equation and the inflection circle, in order to determine the center of curvature of the mass center trajectory for the chassis roll motion. The proposed formulation has been implemented in a Matlab program and several examples allowed its validation in different mechanism configurations.

Keywords: Kinematics, linkages, double wishbone suspension, roll-center, centrodes.

1. INTRODUCTION

The design of a vehicle suspension system is one of the most important aspects of vehicle mechanics, especially with regard to the ride stability and comfort [1]. There are different types of suspension, and in order to obtain the desired project specifications, designers are often faced with optimization problems [2]. One of the most used types of suspensions are double wishbone independent suspensions, especially in high performance vehicles, due to its superior kinematic response.

In designing this type of suspension model, a fundamental parameter is that relating to the motion ratio, which is closely linked to the kinematic properties of the suspension itself, such as instant center of rotation and roll center [3-4]. However, its kinematics is very complicated, as reported in [5-6].

From a kinematic point of view, in vehicle suspension design, some of the most important entities are the abovementioned instant center of rotation and the roll center, especially referring to plane lateral kinematics [7-8]. The determination of these kinematic entities is generally made through the application of the Aronhold-Kennedy theorem [9], but to better understand the behavior of the mechanical system one can refer to different suitable kinematic tools, which have been extensively treated over the years [10-13].

Among these, centrodes can have many applications in the kinematic analysis and synthesis, such as in the field of cam mechanisms [14], linkages [15-16], but also in the vehicle mechanics [17]. On the other hand, together with the centrodes in the analysis and synthesis of mechanisms, some geometric loci of interest can be used, as reported in [18].

In particular, the inflection circle turns out to be very important in the kinematic analysis of plane mechanisms [19-20].

The first phase of kinematic analysis is that of position analysis, which can be carried out by referring to both analytical [21] and graphical [22] methods, with the aim of calculating the instant center of rotation and the centers of curvature, through the application of the Euler-Savary equation.

In this paper, the roll motion analysis of vehicles which are provided of two double wishbone independent suspension mechanisms on the front side, is carried out according to a planar car model that consists of an eight-bar mechanism. Both centrodes are determined and a first curvature analysis is developed. The proposed formulation has been validated by means of several graphical and numerical results.

2. PLANAR CAR MODEL

One major problem in automotive suspension design is of locating the instant center of rotation *IC* between the body of the vehicle and the ground. The problem can be solved by using planar models of the front and rear axles of the vehicle to first locate the front and rear ICs of the vehicle body relative to the ground, as called roll centers. The line connecting these two ICs is the roll axis of the vehicle, the disposition of which relative to the center of mass is critical to the concerning dynamics stability of the vehicle. A two-dimensional vehicle model is composed by a car body and two wheels which are connected by a double-wishbone suspension system as sketched in Fig. 1. A double wishbone suspension is a type of independent suspension system for vehicles that uses two wishbone-shaped arms to control the movement of the wheels. It's also often referred to as a double A-arms. Referring to Fig.1, the wheel 2 is connected to an upper 4 and lower control arm 3, respectively which are attached to the body of vehicle 8. Similarly, to the wheel 5 because the system is symmetrical with respect the axis of the body 8.

The wheels can move up and down independently of each other, thanks to the double wishbone design. This means that double wishbone suspension can provide a smoother ride than other types of suspensions.

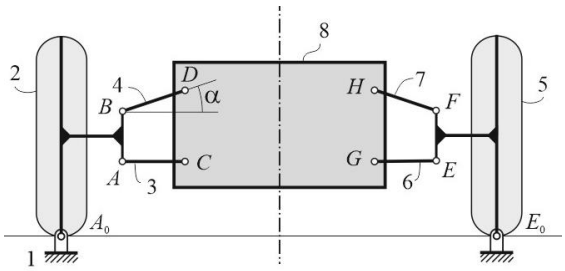

FIGURE 1: PLANAR CAR MODEL

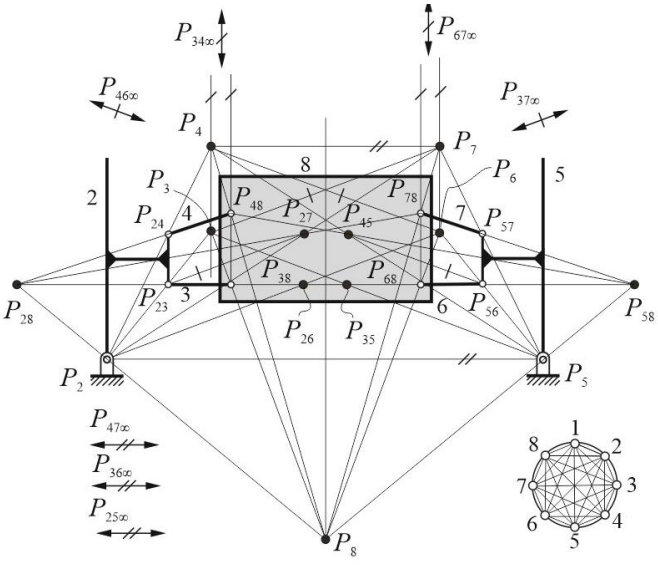

FIGURE 2: ALL ICs AND THE CORRESPONDING AK LINES.

The lines of center or Aronhold-Kennedy lines are lines along which the ICs of the three distinct links are located.

The total number of ICs of a mechanism with *n* links is equals to a combination of *n* taken by 2, as

$$n_{\mathrm{IC}} = \frac{n(n-1)}{2} \tag{1}$$

When $n = 8$ the n_{IC} is equal to 28. Fig.2 show the 8-bar with all its IC$_s$ and all AK lines identified.

Referring to Fig. 2, P_2 and P_5 are the instant centers of rotation (ICs) of left and right wheel contacts points; P_{23} and P_{24} are the ICs of links 2 with respect 3 and 2 with respect 4 respectively; P_{38} and P_{48} are the ICs of links 3 with respect 8 and 4 with respect 8 respectively; P_{56} and P_{57} are the ICs of links 5 with respect 6 and 5 with respect 7 respectively; P_{68} and P_{78} are the ICs of links 6 with respect 8 and 7 with respect 8 respectively.

As shown in Fig. 2, P_{28} can be found with the aid of Aronhold-Kennedy theorem which states that it must lie on the intersection of lines P_{24} - P_{48} and P_{23} - P_{38}, respectively, while, P_{58} must lie on the intersection of lines P_{24} - P_{48} and P_{23} - P_{38}, respectively. Similarly, the roll center P_8 is identified by the intersection of the lines passing through the centers P_2 - P_{28} and $P_5 - P_{58}$, respectively.

3. ROLL MOTION ANALYSIS

Referring to Fig.3, the position analysis is developed by the following three loop-closure equations

$$\mathbf{r}_{2B} + \mathbf{r}_4 + \mathbf{r}_{8b} + \mathbf{r}_7 = \mathbf{r}_1 + \mathbf{r}_{5F} \tag{1}$$

$$\mathbf{r}_{2A} + \mathbf{r}_3 + \mathbf{r}_{8b} + \mathbf{r}_6 = \mathbf{r}_1 + \mathbf{r}_{5E} \tag{2}$$

$$\mathbf{r}_2 + \mathbf{r}_4 + \mathbf{r}_{8h} = \mathbf{r}_3 \tag{3}$$

Consequently, the position vectors $\mathbf{r}_A$, $\mathbf{r}_B$, $\mathbf{r}_C$, $\mathbf{r}_D$, $\mathbf{r}_E$, $\mathbf{r}_F$, $\mathbf{r}_G$, $\mathbf{r}_H$, and $\mathbf{r}_{G8}$, of points *A*, *B*, *C*, *D*, *E*, *F*, *G*, *H* and G_8 are given by

$$\mathbf{r}_A = \mathbf{r}_{2A} \quad \mathbf{r}_B = \mathbf{r}_{2B} \quad \mathbf{r}_C = \mathbf{r}_{2A} + \mathbf{r}_3 \quad \mathbf{r}_D = \mathbf{r}_{2B} + \mathbf{r}_4 \tag{4}$$

$$\mathbf{r}_G = \mathbf{r}_C + \mathbf{r}_{8b} \quad \mathbf{r}_H = \mathbf{r}_D + \mathbf{r}_{8b} \quad \mathbf{r}_E = \mathbf{r}_1 + \mathbf{r}_{5E} \quad \mathbf{r}_F = \mathbf{r}_1 + \mathbf{r}_{5F} \tag{5}$$

$$\mathbf{r}_{G8} = \mathbf{r}_D + \frac{1}{2}\left(\mathbf{r}_{8b} + \mathbf{r}_{8h}\right) \tag{6}$$

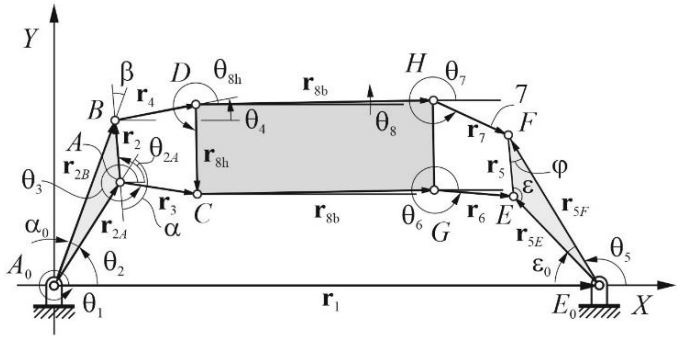

FIGURE 3: VECTOR LOOPS OF 8-BAR MECHANISM.

Thus, each vector $\mathbf{r}_i$ for $i = 1, \ldots, 7$ can be expressed in matrix form with respect to the fixed frame OX_0Y_0 as

$$\mathbf{r}_i = r_i \begin{bmatrix} \cos\theta_i & \sin\theta_i & 1 \end{bmatrix}^T \tag{6}$$

where r_i and θ_i are the magnitude and the counterclockwise angle of vector $\mathbf{r}_i$ respectively, while T indicates the transpose, while r_{8b} and r_{8h} can be expressed as

$$\mathbf{r}_{8b} = r_{8b} \begin{bmatrix} \cos\theta_8 & \sin\theta_8 & 1 \end{bmatrix}^T \tag{7}$$

$$\mathbf{r}_{8h} = r_{8h} \begin{bmatrix} \cos\theta_{8h} & \sin\theta_{8h} & 1 \end{bmatrix}^T \tag{8}$$

where $\theta_{8h} = \left(\theta_8 + \frac{3}{2}\pi\right)$.

Developing Eq. (1) – (3) one has

$$\begin{aligned} r_{2B}\cos(\theta_2 + \alpha_0) + r_4\cos\theta_4 + r_{8b}\cos\theta_8 + r_7\cos\theta_7 &= r_1 + r_{5F}\cos\theta_5 \\ r_{2B}\sin(\theta_2 + \alpha_0) + r_4\sin\theta_4 + r_{8b}\sin\theta_8 + r_7\sin\theta_7 &= r_{5F}\sin\theta_5 \end{aligned} \tag{9}$$

$$\begin{aligned} r_{2A}\cos\theta_2 + r_3\cos\theta_3 + r_{8b}\cos\theta_8 + r_6\cos\theta_6 &= r_1 + r_{5E}\cos(\theta_5 + \varepsilon_0) \\ r_{2A}\sin\theta_2 + r_3\sin\theta_3 + r_{8b}\sin\theta_8 + r_6\sin\theta_6 &= r_{5E}\sin(\theta_5 + \varepsilon_0) \end{aligned} \tag{10}$$

$$\begin{aligned} r_2\cos(\theta_2 + \pi - \alpha) + r_4\cos\theta_4 + r_{8h}\cos\theta_{8h} &= r_3\cos\theta_3 \\ r_2\sin(\theta_2 + \pi - \alpha) + r_4\sin\theta_4 + r_{8h}\sin\theta_{8h} &= r_3\sin\theta_3 \end{aligned} \tag{11}$$

Equations (9 – 11) represent a non-linear system, where r_i, θ_2, $\alpha_0 = \varepsilon_0$, $\alpha = \varepsilon$, $\beta = \varphi$ are given, while the oriented angles θ_3, θ_4, θ_5, θ_6, θ_7, and θ_8 are the unknowns.

This non-linear system has been solved by using the *fsolve* function of Matlab, which can give the solution without iterations. In particular, the *fsolve* function is able to find all the independent variables, such those for which all the functions are zero or near zero. Thus, the choice of the initial configuration of the mechanism is important in order to obtain a right result.

4. ROLL CENTER CENTRODES

In general, the relative planar motion between two rigid bodies can be reproduced by the pure rolling of two curves that take the role of centrodes, which are traced by the instantaneous center of rotation on their corresponding planes. If one of the two rigid bodies is fixed, a pair of fixed and moving centrodes can be obtained.

In particular, referring to Fig.4, the fixed centrode λ is the path traced by the instantaneous center of rotation P_8 of the body 8 with respect the fixed frame OXY, while the moving centrode l is the path traced by P_8 with respect the moving frame $O_8x_8y_8$ that is attached to link 8.

According to the Aronhold-Kennedy theorem, the fixed centrode λ of the body can be expressed by

$$\mathbf{r}_{8\lambda} = \mathbf{r}_{P8} = \begin{bmatrix} \dfrac{x_{P28}\left(x_{E0}y_{P58} - x_{P58}y_{E0}\right)}{y_{P28}\left(x_{E0} - x_{P58}\right) - x_{P28}\left(y_{E0} - y_{P58}\right)} \\ \\ \dfrac{y_{P28}\left(x_{E0}y_{P58} - x_{P58}y_{E0}\right)}{y_{P28}\left(x_{E0} + x_{P58}\right) - x_{P28}\left(y_{E0} - y_{P58}\right)} \end{bmatrix} \tag{12}$$

where x_{P28} and y_{P28} can be found as the intersection of lines P_{24} - P_{48} and P_{23} - P_{38}, one has

$$\mathbf{r}_{P28} = \begin{bmatrix} \dfrac{\left(x_B - x_D\right)\left[x_A\left(y_B - y_C\right) + x_C\left(y_A - y_B\right)\right] - \left(y_B - y_D\right)x_B\left(x_A - x_C\right)}{\left(x_B - x_D\right)\left(y_A - y_C\right) - \left(y_B - y_D\right)\left(x_A - x_C\right)} \\ \\ \dfrac{y_B\left(y_A - y_C\right) - \left(y_B - y_D\right)\left[y_A\left(x_B - x_C\right) + y_C\left(x_A - x_B\right)\right]}{\left(x_B - x_D\right)\left(y_A - y_C\right) - \left(y_B - y_D\right)\left(x_A + x_C\right)} \end{bmatrix} \tag{13}$$

while x_{P58} and y_{P58} can be found on the intersection of lines P_{24} - P_{48} and P_{23} - P_{38}, as

$$\mathbf{r}_{P58} = \begin{bmatrix} \dfrac{\left(x_F - x_H\right)\left[x_E\left(y_F - y_G\right) + x_G\left(y_E - y_B\right)\right] - \left(y_B - y_H\right)x_F\left(x_E - x_G\right)}{\left(x_F - x_H\right)\left(y_E - y_G\right) - \left(y_F - y_H\right)\left(x_E - x_G\right)} \\ \\ \dfrac{y_F\left(y_E - y_G\right) - \left(y_F - y_H\right)\left[y_E\left(x_F - x_G\right) + y_G\left(x_E - x_F\right)\right]}{\left(x_F - x_H\right)\left(y_E - y_G\right) - \left(y_F - y_H\right)\left(x_E + x_G\right)} \end{bmatrix} \tag{14}$$

The moving centrode l takes the form

$$\mathbf{r}_{8l} = \begin{bmatrix} \overline{P_8C}\cos\left(\theta_{P8C} - \theta_8\right) & \overline{P_8C}\sin\left(\theta_{P8C} - \theta_8\right) & 1 \end{bmatrix}^T \tag{15}$$

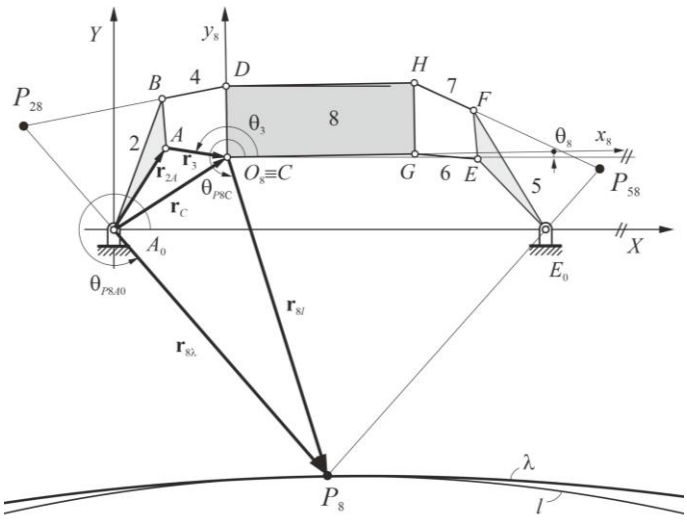

FIGURE 4: FIXED λ AND MOVING CENTRODE l

where

$$\overline{P_8C} = \sqrt{\left(x_{P8} - x_C\right)^2 + \left(y_{P8} - y_C\right)^2} \tag{16}$$

$$\theta_{P8C} = \tan^{-1}\left(\frac{y_{P8} - y_C}{x_{P8} - x_C}\right) \tag{17}$$

In order to express both moving centrode l of link 8 with respect to OXY, the position vector $\mathbf{r}^*_{Pi}$ of a generic point P with respect to the moving frame $\Omega_i x_i y_i$ can be expressed as

$$\mathbf{r}^*_{Pi} = r^*_{Pi}\begin{bmatrix}\cos\theta_i & \sin\theta_i & 1\end{bmatrix}^T \tag{18}$$

and thus, the position vector $\mathbf{r}_{Pi}$ of P in OXY can be given

$$\mathbf{r}_{Pi} = \mathbf{T}_8\,\mathbf{r}^*_{Pi} \tag{19}$$

being $\mathbf{T}_8$ the following transformation matrix by the moving frame $O_i x_i y_i$ to OX_0Y_0

$$\mathbf{T}_8 = \begin{bmatrix}\cos\theta_8 & -\sin\theta_8 & x_{O8}\\ \sin\theta_8 & \cos\theta_8 & y_{O8}\\ 0 & 0 & 1\end{bmatrix} \tag{22}$$

where θ_i is the counterclockwise rotation angle of $O_i x_i y_i$ with respect to OXY, while x_{Oi} and y_{Oi} are the Cartesian coordinates of the origin O_i in the same fixed frame.

The coordinates ($x_{O\lambda}$, $y_{O\lambda}$) of a point of the osculating circle for the fixed centrode λ can be found as the intersection of the following two straight lines

$$\begin{aligned} y - y_{M1} &= -\frac{1}{m_1}\left(x - x_{M1}\right)\\ y - y_{M2} &= -\frac{1}{m_2}\left(x - x_{M2}\right)\end{aligned} \tag{21}$$

Thus, one has

$$\mathbf{r}_{O\lambda} = \begin{bmatrix} -\dfrac{\left(x_{M1}m_2 - x_{M2}m_1\right) + m_1m_2\left(y_{M1} - x_{M2}\right)}{m_1 - m_2}\\[2ex] \dfrac{x_{M1} - x_{M2} + y_{M1}m_1 - x_{M2}m_2}{m_1 - m_2}\end{bmatrix} \tag{22}$$

where

$$m_1 = \frac{y_{P8}^{(i-1)} - y_{P8}^{(i)}}{x_{P8}^{(i-1)} - x_{P8}^{(i)}} \qquad m_2 = \frac{x_{P8}^{(i+1)} - x_{P8}^{(i)}}{y_{P8}^{(i+1)} - y_{P8}^{(i)}} \tag{23}$$

$$\begin{aligned} x_{M1} &= \frac{x_{P8}^{(i-1)} + x_{P8}^{(i)}}{2}, \quad y_{M1} = \frac{y_{P8}^{(i-1)} + y_{P8}^{(i)}}{2}\\ x_{M2} &= \frac{x_{P8}^{(i+1)} + x_{P8}^{(i)}}{2}, \quad y_{M2} = \frac{y_{P8}^{(i+1)} + y_{P8}^{(i)}}{2}\end{aligned} \tag{24}$$

The curvature radius r_λ of the fixed centrode λ can be determined as follows

$$r_\lambda = \sqrt{\left(x_{O\lambda} - x_{M1}\right)^2 + \left(y_{O\lambda} - y_{M1}\right)^2} \tag{25}$$

The same approach can be also applied to achieve the curvature radii of the moving centrode l and the trajectory of the mass center G_8, respectively.

Thus, the diameter Δ of the inflection circle $\mathcal{I}$ can be determined by taking into what follows

$$-\frac{1}{\Delta} = \frac{1}{r_\lambda} - \frac{1}{r_l} \qquad \Delta = \frac{r_\lambda r_l}{r_\lambda - r_l} \tag{26}$$

Consequently, the equation of $\mathcal{I}$ takes the form

$$\left(x - x_{O\mathcal{I}}\right)^2 + \left(y - y_{O\mathcal{I}}\right)^2 = \left(\frac{\Delta}{2}\right)^2 \tag{27}$$

where the Cartesian coordinates $x_{O\mathcal{I}}$ and $y_{O\mathcal{I}}$ of the center are expressed as function of the angle ϑ by

$$\begin{aligned} x_{O\mathcal{I}} &= x_{P8} - \frac{\Delta}{2}\cos\vartheta, \quad y_{O\mathcal{I}} = x_{P8} - \frac{\Delta}{2}\sin\vartheta\\ \vartheta &= \tan^{-1}\frac{y_{P8} - y_{O\lambda}}{x_{P8} - x_{O\lambda}}\end{aligned} \tag{28}$$

Finally, the center of curvature Ω_{G8} of the path traced by the mass center G_8 of the chassis, can be obtained from the Euler-Savary equation, as follows

$$\Omega_{G8}G_8 = \frac{\left(P_8G_8\right)^2}{G'_8G_8} \tag{29}$$

where G'_8 is the corresponding point of G_8 that lies on the inflection circle.

5. CENTRODES: MECHANICAL GENERATION

Referring to Figs. 5 and 6, a suitable mechanism with 18 members and 1 d.o.f. is proposed to generate mechanically or by using any CAD-software, both centrodes, according to the direct and inverse planar motion of the chassis with respect to the

ground and vice versa. This mechanism has been derived by the planar car model of Fig. 1, where the links 3 and 4 on the left and the links 6 and 7 on the right, have been extended to guide the P_{28} and P_{58} moving revolute joints, which have also the role of ICs and guide the links 14 and 16 by means of both prismatic joints in P_2 and P_5, respectively. The revolute joint laying in the roll center P_8 is moved to trace the fixed centrode and likewise, the moving centrode can be traced by using the inverse mechanism of Fig. 6, where the chassis 8 is assumed as fixed frame and the ground link 1 becomes the coupler link.

Referring to Fig.5, the total number of ICs of a mechanism with n =18 links is given by

$$n_{\text{dof}} = 3(n-1) - 2l - h = 3(18-1) - (2\cdot 17 + 4\cdot 4) = 1 \text{ d.o.f.} \quad (30)$$

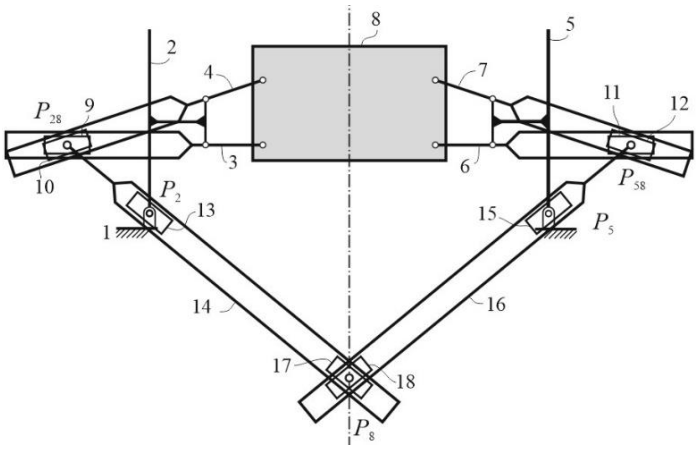

FIGURE 5: 18-BAR MECHANISM: DIRECT MOTION.

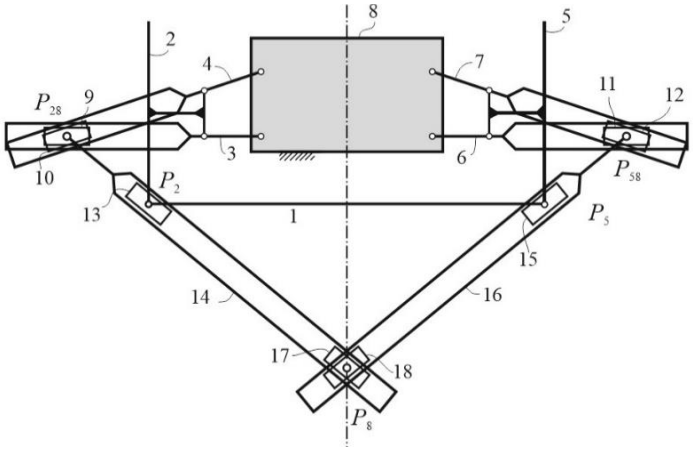

FIGURE 6: 18-BAR MECHANISM: INVERSE MOTION

6. GRAPHICAL AND NUMERICAL RESULTS

The proposed formulation has been implemented in Matlab and validated by means of significant examples.

In particular, Fig. 7 shows the eight-bar mechanism of the planar car model of Fig. 1 for θ_2 = 55.4 deg, ω_2 = 1 r/s, r_2 =r_5 = 200 u, r_{2A} = r_3 = r_{5E} = r_6 = 400 u, r_{2B} = r_{5F} = 581.8 u, r_4 = 4561.9 u, r_{8b} = 800 u, r_{8h} = 358 u, while Fig. 8 and 9 show different examples for θ_2 = 61.2 deg and θ_2 = 57.2 deg., respectively.

In particular, the moving centrode is internal to the fixed one and the inflection circle $\mathcal{I}$ is located on the l side.

7. CONCLUSIONS

The roll motion analysis of vehicles which are provided of two double wishbone independent suspension mechanisms on the front side, has been formulated by including the determination of the fixed and moving centrodes of the chassis, which can be also obtained in mechanical way.

Moreover, a first curvature analysis has been carried out, in order to determine the center of curvature of the mass center trajectory. Several examples validated the proposed formulation.

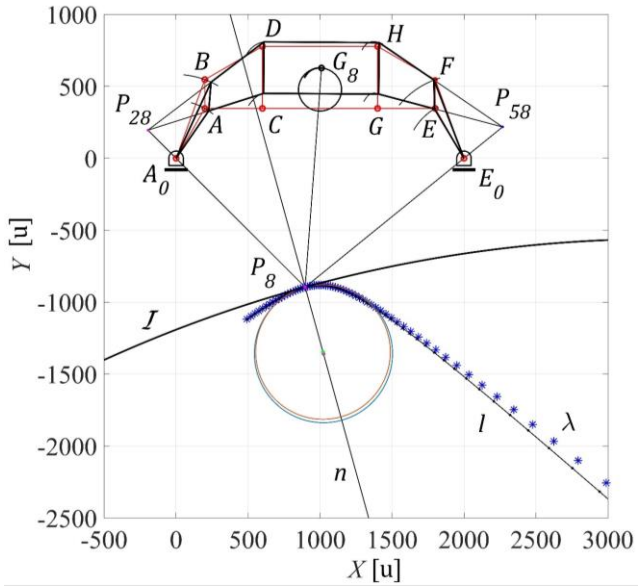

FIGURE 7. 8-BAR MECHANISM FOR θ_2 = 55.4 DEG.

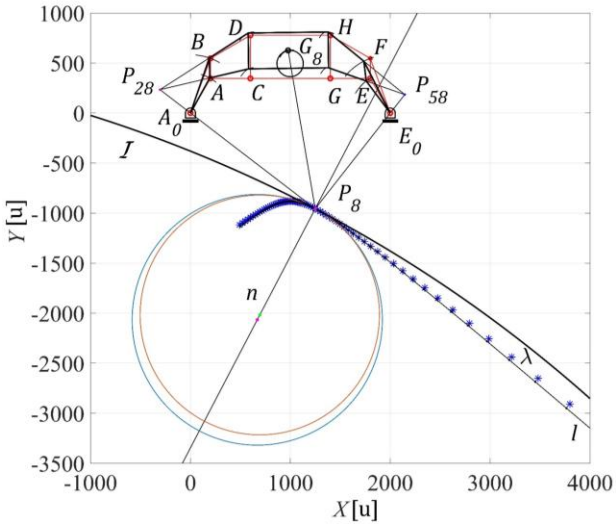

FIGURE 8. 8-BAR MECHANISM FOR θ_2 = 61.2 DEG.

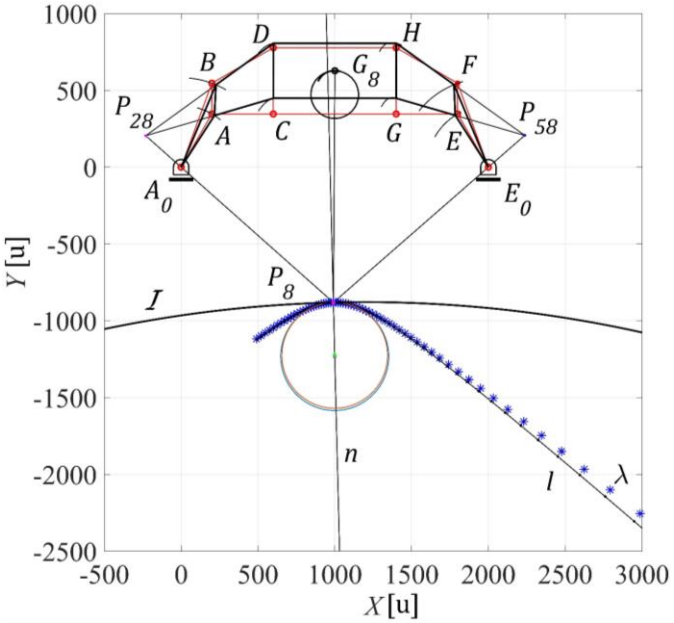

FIGURE 9: 8-BAR MECHANISM FOR θ_2 = 57.2 DEG.

ACKNOWLEDGEMENTS

This study was carried out within the MOST – Sustainable Mobility Center and received funding from the European Union Next-Generation EU (PIANO NAZIONALE DI RIPRESA E RESILIENZA (PNRR) – MISSIONE 4 COMPONENTE 2, INVESTIMENTO 1.4 – D.D. 1033 17/06/2022, CN00000023). This manuscript reflects only the authors' views and opinions, neither the European Union nor the European Commission can be considered responsible for them.

REFERENCES

[1] Mahmoodi-Kaleibar, M. *et al.* (2013). Optimization of suspension system of off-road vehicle for vehicle performance improvement. *J. of Central S. University*, 20 (4), pp. 902–910.

[2] Simionescu, P.A., Beale, D. (2002). Synthesis and analysis of the five-link rear suspension system used in automobiles. *Mech. and Machine Theory*, 37(9), pp. 815–832.

[3] Bucchi, F. and Lenzo, B. (2022). Analytical derivation and analysis of vertical and lateral installation ratios for swing axle, McPherson and double wishbone suspension architectures. *Actuators*, 11 (8), p. 229.

[4] Kodati, M. and Bandyopadhyay, S. (2013). Kinematic analysis of the double wishbone suspension system, Proc. of the 1st Int. and 16th National Conference on Machines and Mechanisms (iNaCoMM2013), IIT Roorkee, India.

[5] Unlusoy, Y. S. (2020). Kinematic modelling and simulation of a special double wishbone suspension and steering system for heavy vehicles, 10th Int. Automotive Technologies Congress, OTEKON 2020.

[6] Uchida, T. and McPhee, J. (2012). Driving simulator with double-wishbone suspension using efficient block-triangularized kinematic equations. *Multibody System Dynamics*, 28(4), pp. 331–347.

[7] Morse, P. and Starkey, J.M. (1996). A force-based roll center model for vehicle suspensions. SAE Technical Paper 962536 Series, 12 pages.

[8] Lee, J.-K. and Shim, J.-K. (2006). Kinematic method for roll center analysis of a half-car model with variable wheel tread width. 30th *Annual Mechanisms and Robotics Conference*, Vol. 2: Parts A and B.

[9] Simionescu, P.A., Talpasanu, I. and Di Gregorio, R. (2010). "Instant-center based force transmissivity and singularity analysis of planar linkages. *J. of Mechanisms and Rob.*, 2 (2).

[10] Hartenberg, R.S. and Denavit, J. (1964). *Kinematic synthesis of linkages*. McGraw-Hill.

[11] Di Benedetto, A. and Pennestrì E. (1991). *Introduzione alla cinematica dei meccanismi*. Milano: Casa Editrice Ambrosiana.

[12] Hunt, K.H. (1990). *Kinematic geometry of mechanisms*. Oxford: Clarendon Press.

[13] Norton, R.L. (2020). *Design of Machinery: An introduction to the synthesis and analysis of mechanisms and machines*. New York, NY: McGraw-Hill Education.

[14] Figliolini, G., Rea, P., Angeles, J. (2006). The pure-rolling cam-equivalent of the Geneva mechanism. *Mechanism and Machine Theory*, 41 (11), pp. 1320-1335.

[15] Figliolini, G. and Pennestrì, E. (2015). Synthesis of quasi-constant transmission ratio planar linkages. *Journal of Mechanical Design*, 137 (10).

[16] Figliolini, G., Lanni, C. and Sorli, M. (2022). Kinematic analysis and centrodes between rotating tool with reciprocating motion and workpiece. *Mechanisms and Machine S.*, pp.54–60.

[17] Figliolini, G., Lanni, C. and Angeles, J. (2020). Kinematic analysis of the planar motion of vehicles when traveling along Tractrix curves. *J. of Mech. and Rob.*, 12(5).

[18] Figliolini G., Lanni C. (2018). Geometric loci for the kinematic analysis of planar mechanisms via the instantaneous geometric invariants, MEDER: Proc. of the 4th IFT0MM Symposium on Mechanism Design, Gasparetto A. & Ceccarelli M. (Eds.), Springer, Cham, pp.184-192.

[19] Figliolini G., Lanni C., Tomassi L. (2022). First and Second Order Centrodes of Slider-Crank Mechanisms by Using Instantaneous Invariants, In: Altuzarra O., Kecskeméthy A. (Eds.): 18th International Symposium on Advances in Robot Kinematics, ARK 2022, Springer Proc. in Advanced Robotics, Volume 24 SPAR, p. 303 – 310.

[20] Figliolini G., Lanni C., Tomassi L. (2020). Kinematic Analysis of Slider – Crank Mechanisms via the Bresse and Jerk's Circles. Carcaterra A., Paolone A., Graziani G. (eds) Proc. of XXIV AIMETA 2019. Lecture Notes in Mechanical Engineering. Springer, Cham. pp. 278-284.

[21] Dhingra, A.K., Almadi, A.N. and Kohli, D. (1999). A Groebner-Sylvester hybrid method for closed-form displacement analysis of mechanisms. *J. of Mechanical Design*, 122(4), pp. 431–438.

[22] Pennock, G.R. and Kinzel, E.C. (2003). Path curvature of the single flier eight-bar linkage. *J. of Mechanical Design*, 126(3), pp. 470–477.